American Mineralogist, Volume 99, pages 625–632, 2014

Mathesiusite, $K_5(UO_2)_4(SO_4)_4(VO_5)(H_2O)_4$, a new uranyl vanadate-sulfate from Jáchymov, Czech Republic

Jakub Plášil[1,*], František Veselovský[2], Jan Hloušek[3], Radek Škoda[4], Milan Novák[4], Jiří Sejkora[5], Jiří Čejka[5], Pavel Škácha[6] and Anatoly V. Kasatkin[7]

[1]Institute of Physics ASCR, v.v.i., Na Slovance 2, CZ-182 21, Praha 8, Czech Republic
[2]Czech Geological Survey, Geologická 6, CZ-152 00, Praha 5, Czech Republic
[3]U Roháčových kasáren 24, CZ-100 00, Praha 10, Czech Republic
[4]Department of Geological Sciences, Faculty of Science, Masaryk University, Kotlářská 2, CZ-611 37, Brno, Czech Republic
[5]Department of Mineralogy and Petrology, National Museum, Cirkusová 1740, CZ-193 00, Praha 9, Czech Republic
[6]Mining Museum Příbram, nám. Hynka Kličky 293, 261 01, Příbram VI, Czech Republic
[7]V/O "Almazjuvelirexport", Ostozhenka Street, 22, block 1, 119034 Moscow, Russia

Abstract

Mathesiusite, $K_5(UO_2)_4(SO_4)_4(VO_5)(H_2O)_4$, a new uranyl vanadate-sulfate mineral from Jáchymov, Western Bohemia, Czech Republic, occurs on fractures of gangue associated with adolfpateraite, schoepite, čejkaite, zippeite, gypsum, and a new unnamed K-UO_2-SO_4 mineral. It is a secondary mineral formed during post-mining processes. Mathesiusite is tetragonal, space group $P4/n$, with the unit-cell dimensions a = 14.9704(10), c = 6.8170(5) Å, V = 1527.78(18) Å^3, and Z = 2. Acicular aggregates of mathesiusite consist of prismatic crystals up to ~200 μm long and several micrometers thick. It is yellowish green with a greenish white streak and vitreous luster. The Mohs hardness is ~2. Mathesiusite is brittle with an uneven fracture and perfect cleavage on {110} and weaker on {001}. The calculated density based on the empirical formula is 4.02 g/cm^3. Mathesiusite is colorless in fragments, uniaxial (–), with ω = 1.634(3) and ε = 1.597(3). Electron microprobe analyses (average of 7) provided: K_2O 12.42, SO_3 18.04, V_2O_5 4.30, UO_3 61.46, H_2O 3.90 (structure), total 100.12 (all in wt%). The empirical formula (based on 33 O atoms pfu) is: $K_{4.87}(U_{0.99}O_2)_4(S_{1.04}O_4)_4(V_{0.87}O_5)(H_2O)_4$. The eight strongest powder X-ray diffraction lines are [d_{obs} in Å (*hkl*) I_{rel}]: 10.64 (110) 76, 7.486 (200) 9, 6.856 (001) 100, 6.237 (101) 85, 4.742 (310) 37, 3.749 (400) 27, 3.296 (401) 9, and 2.9409 (510) 17. The crystal structure of mathesiusite was solved from single-crystal X-ray diffraction data and refined to R_1 = 0.0520 for 795 reflections with $I > 3\sigma(I)$. It contains topologically unique heteropolyhedral sheets based on $[(UO_2)_4(SO_4)_4(VO_5)]^{5-}$ clusters. These clusters arise from linkages between corner-sharing quartets of uranyl pentagonal bipyramids, which define a square-shaped void at the center that is occupied by V^{5+} cations. Each pair of uranyl pentagonal bipyramids shares two vertices of SO_4 tetrahedra. Each SO_4 shares a third vertex with another cluster to form the sheets. The K^+ cations are located between the sheets, together with a single H_2O group. The corrugated sheets are stacked perpendicular to **c**. These heteropolyhedral sheets are similar to those in the structures of synthetic uranyl chromates. Raman spectral data are presented confirming the presence of UO_2^{2+}, SO_4, and molecular H_2O.

Keywords: Mathesiusite, new mineral, uranyl sulfate, vanadate, crystal structure, Raman spectroscopy, oxidation zone, Jáchymov

Introduction

In the course of study of the new mineral adolfpateraite, $K(UO_2)(SO_4)(OH)(H_2O)$ (Plášil et al. 2012), we discovered another new unnamed uranyl mineral that is closely associated with adolfpateraite. Here we provide a description of this new mineral, mathesiusite, which is another uranyl sulfate from the Jáchymov deposit. It has the chemical composition, $K_5(UO_2)_4(SO_4)_4(VO_5)(H_2O)_4$, and a unique structure topology among known structures of uranyl minerals. The topology and chemical composition of the new mineral are discussed using the bond-valence approach.

The new mineral honors an evangelical (Lutheran) priest and theologian, Johannes Mathesius (1504–1565), a student of theology and philosophy under the supervision of the famous Martin Luther. From 1532 until his death, Mathesius lived and served in Jáchymov, first as a teacher at the Latin lyceum, then as a pastor in one of the first evangelic churches in the world. He provided significant gains to the natural sciences (especially mineralogy), his most important piece of work being "Sarepta oder Bergpostil," printed in 1562. The new mineral mathesiusite and the name has been approved by the Commission on New Minerals, Nomenclature and Classification of the International Mineralogical Association (IMA 2013-046). The holotype specimen is deposited in the collections of the Department of Mineralogy and Petrology of the National Museum in Prague, under the catalog number P1P 7/2013.

* E-mail: plasil@fzu.cz

Occurrence

Mathesiusite was found in an old mine adit on the Geschieber vein, at the fifth level of the Svornost (Einigkeit) mine, Jáchymov ore district, Western Bohemia, Czech Republic (50°22′21.136″N, 12°54′46.150″E). The Jáchymov ore district presents classic examples of Ag-As-Bi-Co-Ni-U hydrothermal vein type deposits (Ondruš et al. 2003). More than 420 minerals have been found at the Jáchymov ore district, including the rich assemblage of supergene minerals (see Ondruš et al. 1997, 2003) that yielded many new mineral species. Mathesiusite appears to be an extremely rare mineral, occurring only on a few specimens. The matrix of the specimens consists of gangue or fragments of surrounding rocks without primary U mineralization. Secondary minerals occur on the surfaces of the specimens. Gypsum, schoepite, čejkaite, adolfpateraite, and a new K-UO_2-SO_4 mineral were found in close association. Neither primary uranium minerals nor any sulfides were observed in the gangue samples. Mathesiusite is a mineral of the supergene origin, connected to the acid-mine drainage (AMD) in the underground of the former mine adit.

Physical and optical properties

Mathesiusite occurs as isolated radiating and fan-shaped aggregates of thin prismatic to acicular crystals, reaching up to 0.2 mm in length (along the **c** axis). The mineral is usually associated on the matrix with adolfpateraite; mathesiusite commonly partially overgrows adolfpateraite aggregates (Fig. 1). Mathesiusite is yellowish green; crystals are translucent to transparent with a vitreous luster. It has greenish white streak. Crystals are brittle, with perfect cleavage on {110} and weaker on {001}, and have uneven fracture. Morphological description is very difficult due to the very small size of mathesiusite crystals and their brittleness. The Mohs hardness is ~2. The direct determination of density could not been done because of the extremely small quantity of material for study. A density of 4.018 g/cm^3 was calculated based on the unit-cell dimensions from single-crystal X-ray data and chemical composition obtained from electron microprobe results. Mathesiusite shows strong yellowish green fluorescence both in long- and short-wave UV radiation. The mineral is colorless in fragments under the microscope, uniaxial negative, with ω = 1.634(3), ε = 1.597(3). Gladstone-Dale compatibility [$1 - (K_P/K_C) = 0.070$], as calculated from the empirical formula using the density derived from the single-crystal unit cell, is rated as fair. Considering the ideal formula and optical properties the Gladstone-Dale compatibility is 0.025, rated as excellent.

Figure 1. Greenish-yellow radiating aggregate of mathesiusite composed of fine, needle-like crystals in association with bright-yellow adolfpateraite on reddish gangue. FOV 3.0 mm. Photo: P. Škácha.

Chemical composition

Quantitative chemical analyses of mathesiusite were obtained using a Cameca SX100 electron microprobe (WDS mode, 15 kV, 4 nA, and 15 μm beam diameter) at the Department of Geological Sciences, Masaryk University in Brno, Czech Republic. The following X-ray lines and standards were used: *K*α lines: S ($SrSO_4$), K (sanidine), V ($ScVO_4$), *M*β lines: U (uranophane). Other elements, such as Na, Ca, or Mg were also sought, but were below the detection limits of these elements (~0.1 wt% with the analytical conditions used). The peak counting times (CT) were 10–20 s and the counting time for each background point was 50% of the peak CT. X-ray matrix effects were corrected using the PAP correction-routine (Pouchou and Pichoir 1985). Despite the soft analytical conditions used, part of the potassium content was volatilized and escaped the specimen under the beam during the analysis (which was followed by the intensity loss of emitted X-rays). Therefore, an extrapolation of the polynomial (quadratic) fit of counts to time t = 0 s was used to obtain the content of potassium before the loss (see Discussion).

Mathesisusite is an uranyl vanadate-sulfate mineral characterized by an K:U:S ratio of 1.25:1:1. The chemical composition of mathesiusite is quite homogeneous with slight variance in the K content (Table 1). The empirical formula is $K_{4.87}(U_{0.99}O_2)_4(S_{1.04}O_4)_4(V_{0.87}O_5)(H_2O)_4$ (based on 33 O apfu) H_2O content calculated by stoichiometry obtained from the structure refinement). The simplified formula is $K_5(UO_2)_4(SO_4)_4(VO_5)(H_2O)_4$, which requires 12.64 K_2O, 4.88 V_2O_5, 17.19 SO_3, 61.42 UO_3, 3.87 H_2O, total 100.00 wt%.

Raman microspectroscopy

The Raman spectrum of mathesiusite was recorded on a Thermo-Scientific DXR Raman microscope interfaced to an Olympus microscope (objective 50×) in the 50–3150 cm^{-1} spectral region with ~5 cm^{-1} spectral resolution. The power of the frequency-stabilized single mode diode laser (780 nm) impinging on the sample ranged from 4 to 8 mW. This wavelength was selected since a strong fluorescence occurred, while the green laser (532 nm) was used. The spectrometer was calibrated by a software-controlled calibration procedure (within Omnic 8 software) using multiple

Table 1. Results of electron microprobe analyses (in wt%) of mathesiusite

	Mean (n = 7)	Range	S.D.
K_2O	12.42	12.09–12.71	0.29
SO_3	18.04	17.05–18.56	0.58
V_2O_5	4.30	4.10–4.68	0.24
UO_3	61.46	58.29–63.77	2.07
H_2O	3.90*		
Total	100.12		
	Calculated on an 33 O apfu		
K	4.87		
S^{6+}	4.16		
V^{5+}	0.87		
U^{6+}	3.97		
H_2O	4.00		

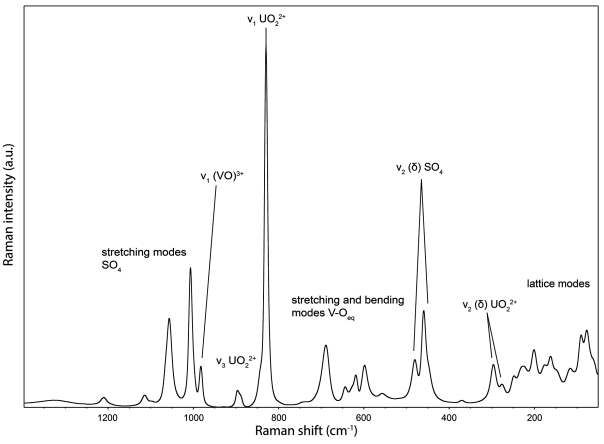

FIGURE 2. Raman spectrum of mathesiusite measured on {110} face with depolarized laser.

neon emission lines (wavelength calibration), multiple polystyrene Raman bands (laser frequency calibration), and standardized white light sources (intensity calibration). Spectral manipulation such as background correction and band-component analysis was done with Omnic 8 software.

The dominant features in the Raman spectrum of mathesiusite are SO_4^{2-} and UO_2^{2+} stretching vibrations (Fig. 2). Features in the high-energy region (O-H stretching modes) could not be measured owing to the restricted capabilities of the spectrometer. Interpretation of the spectrum followed the assignments of Knyazev (2000) and Chernorukov et al. (2000).

The vibration of the highest intensity at 830 cm^{-1} with a shoulder at 844 cm^{-1} is assigned to the ν_1 symmetric stretching vibration of $(UO_2)^{2+}$. The approximate U-O bond lengths of the uranyl ion inferred from these frequencies, according to the empirical relations provided by Bartlett and Cooney (1989), are 1.78 and 1.76 Å, respectively. Antisymmetric stretching modes (ν_3) of uranyl were observed at 888 and 896 cm^{-1}. Corresponding inferred U-O bond lengths is 1.79 Å. For comparison, the U-O bond-lengths that were obtained from the single-crystal X-ray diffraction data are 1.75 and 1.77 Å. Split ν_2 (δ) UO_2^{2+} doubly degenerate bending vibrations are at 276 and 248 cm^{-1}. The weak Raman bands at 598, 557, 480, and 370 cm^{-1} may correspond to ν (U-O_{eq}) modes (Knyazev 2000; Chernorukov et al. 2000), but some of them may also coincide with SO_4 and ν (V-O_{eq}) bending modes.

The stretching vibrations of the sulfate tetrahedral occur in the Raman spectrum of mathesiusite at around ~1200 cm^{-1}. The vibrations s of medium intensity at 1007 and 1210 cm^{-1} are assigned to the ν_1 symmetric stretching vibration of SO_4; triply degenerate ν_3 antisymmetric stretching vibrations occur at 1114 and 1210 cm^{-1}. The band at 1329 cm^{-1} may be attributed to an overtone or a combination band; the triply degenerate ν_4 (δ) bending mode were assigned to bands at 598, 619, and 644 cm^{-1} and ν_2 (δ) doubly degenerate bending mode to those at 447 (shoulder), 460, and 480 cm^{-1}. However, some of these vibration bands may also coincide with ν (U-O_{eq}) and ν (V-O_{eq}) vibrations, which usually have a relatively low intensity (Chernorukov et al. 2000; Knyazev 2000).

The symmetric ν_1 (V-O) stretching mode was assigned to the peak at 982 cm^{-1} (Fig. 2). The following weak bands may also correspond to stretching and bending V-O_{eq} vibrations: 742, 619, 557 cm^{-1} and some bands in the region of lattice modes; some may coincide with SO_4^{2-} bending and ν (U-O_{eq}) vibrations (598, 557, 480, 370 cm^{-1}) (Chernorukov et al. 2000; Knyazev 2000).

TABLE 2. X-ray powder diffraction data for mathesiusite from Jáchymov

I_{obs}	d_{obs}	d_{calc}	I_{calc}	h	k	l	I_{obs}	I_{calc}	d_{obs}	d_{calc}	h	k	l
76	10.64	10.59	82	1	1	0	4	<1	2.4038	2.4043	5	3	1
9	7.486	7.488	5	2	0	0	4	6	2.3713	2.3680	6	2	0
100	6.856	6.835	73	0	0	1	3	<1	2.3448	2.3447	6	0	1
85	6.237	6.218	100	1	0	1	2	2	2.3179	2.3164	6	1	1
7	5.727	5.743	5	1	1	1	1	1	2.2212	2.2274	1	1	3
3	5.301	5.295	18	2	2	0	4	1	2.2054	2.2130	5	4	1
5	5.096	5.048	2	2	0	1	4	17	2.1541	2.1571	2	5	2
4	4.800	4.784	1	1	2	1	2	14	2.1211	2.1222	6	3	1
37	4.742	4.736	43	3	1	0	1	7	2.0793	2.0769	4	6	0
4	4.196	4.186	15	2	2	1	1	4	2.0434	2.0418	7	0	1
3	3.893	3.893	2	1	3	1	1	4	1.9892	1.9872	4	6	1
27	3.749	3.744	<1	4	0	0	1	7	1.9700	1.9665	7	3	0
4	3.554	3.550	34	3	2	1	3	3	1.9336	1.9302	4	5	2
3	3.529	3.530	4	3	3	0	4	6	1.8726	1.8721	8	0	0
5	3.354	3.349	8	4	2	0	1	14	1.8680	1.8691	6	3	2
2	3.334	3.332	40	1	0	2	1	5	1.8125	1.8135	7	0	2
9	3.296	3.284	<1	4	0	1	1	7	1.8062	1.8056	8	0	1
2	3.212	3.208	17	4	1	1	1	2	1.7946	1.7926	4	7	1
7	3.138	3.136	15	3	3	1	7	10	1.6753	1.6723	5	6	2
4	3.014	3.007	18	4	2	1	3	3	1.6303	1.6321	4	7	2
17	2.9409	2.9372	2	5	1	0	2	5	1.6096	1.6073	3	1	4
5	2.8219	2.8200	5	3	0	2	3	3	1.5753	1.5787	3	9	0
3	2.7768	2.7713	<1	1	3	2	1	3	1.5383	1.5382	3	9	1
5	2.7302	2.7435	1	4	3	1	1	1	1.4951	1.4961	9	0	2
3	2.7049	2.6986	12	1	5	1	<1	2	1.4545	1.4560	10	1	1
4	2.6472	2.6475	<1	4	4	0	1	4	1.4453	1.4464	8	0	3
2	2.5745	2.5760	10	2	5	1	1	2	1.4214	1.4228	9	5	1
2	2.5661	2.5685	9	5	3	0	1	1	1.3294	1.3300	11	1	1
2	2.4939	2.4961	1	6	0	0	2	<1	1.2494	1.2481	0	12	0
		2.4851	12	4	1	2							
		2.4851	9	1	4	2							

X-RAY CRYSTALLOGRAPHY AND DETERMINATION OF THE CRYSTAL STRUCTURE

Powder diffraction

The powder diffraction data of mathesiusite (Table 2) were obtained using a PANalytical Empyrean powder diffractometer with a Cu X-ray tube (operated at 45 kV, 40 mA) and PIXcel^{3D} solid-state detector equipped with the curved primary Göbel mirror providing the focused X-ray beam for the Debye-Scherrer geometry. A small portion of the pulverized mathesiusite crystals were loaded into a glass capillary to avoid preferred orientation effects, which were preliminary confirmed using Bragg-Brentano geometry. The preferred orientation is due to the excellent cleavage of mathesiusite crystals. The powder data were collected from 3 to 90° 2θ with a step size 0.013° 2θ and a counting time of 1 s per step. The accumulation of 40 scans was performed to increase the intensity statistics and peak-to-background ratio. Prior to the data collection the diffractometer was calibrated against a LaB_6 standard. The positions of the diffraction peaks were refined from the powder data using a pseudo-Voigt profile shape function in the High-Score program (PANalytical B.V.). The unit-cell parameters were refined using the Checkcell program (LMGP-Suite 2004; Laugier and Bochu 2004) based on the refined positions of the 62 observed fitted diffraction peaks and the *hkl* indices assigned to those diffraction peaks using the calculated powder pattern (PowderCell software; Kraus and Nolze 1996) from the structure

data (see below). Refined unit-cell parameters for the tetragonal space group $P4/n$ are a = 14.977(3), c = 6.8352(8) Å, and V = 1533.2(8) Å^3.

Single-crystal X-ray diffraction

A crystal of mathesiusite with dimensions 0.07 × 0.02 × 0.02 mm was examined by means of an Oxford Diffraction Gemini single-crystal diffractometer with an Atlas CCD detector using graphite-monochromatized Mo$K\alpha$ radiation from a classical sealed X-ray tube. The unit cell was refined from 1969 reflections by a least-squares algorithm within the CrysAlis software (Agilent Technologies 2012). Rotational scans in ω (frame width 0.8°, counting time 200 s per frame) were adopted to cover the Ewald sphere. From a total of 12 825 reflections, 1861 were unique and 795 observed with the criterion [$I > 3\sigma(I)$]. Data were corrected for background, Lorentz and polarization effects, and an analytical correction for absorption was applied (Clark and Reid 1995). The poor internal residual factor, R_{int} = 0.189, is due to the overlaps from the split (twin) crystal and considerably weak diffraction data. Reduction of the data was performed using the CrysAlis package (CrysAlis RED, Agilent Technologies 2012). A summary of data collection, crystallographic data and refinement is given in Table 3.

The crystal structure of mathesiusite was solved by the charge-flipping method (Oszlányi and Sütő 2004, 2008; Palatinus 2013) implemented in the program Superflip (Palatinus and Chapuis 2007). The structure confirms the chosen space group $P4/n$, which was assigned based on the reflection conditions. The structure obtained was subsequently refined by the full-matrix least-squares algorithm of the Jana2006 software (Petříček et al. 2006) based on F^2. Metal site atoms were refined anisotropically. Hydrogen atoms were not located in the difference-Fourier maps of the electron density. Final atom positions and displacement parameters are listed in Tables 4 and 5. A bond valence analysis (following the procedure of Brown 2002), based on refined interatomic distances (Table 6), is provided in Table 7. (CIF[1] is available.)

Description of the crystal structure

Cation coordination

The asymmetric unit of the mathesiusite structure, which crystallizes in the space-group $P4/n$, contains one U, one S, one V, two K, and nine O atoms. Uranium is strongly bonded to two O atoms, forming the nearly linear uranyl ion, with bond lengths 1.767(13) and 1.748(13) Å (Table 6), matching the characteristic range in values (~1.8 Å) of U^{6+}-O_{Ur} distances in the structures containing hexavalent uranium (Burns et al. 1997; Burns 2005). The uranyl ion is further coordinated by five ligands, O atoms, which are arranged in the equatorial vertices of pentagonal bipyramids (with an average equatorial U-O bond-length of 2.38 Å). Sulfur is coordinated by four O atoms at the distances typical for tetrahedral coordination, ~1.45 Å. Vanadium was found in the mathesiusite structure in square pyramidal coordination, bonded strongly to one O atom at the distance of 1.62 Å (vanadyl bond) and four O atoms at the distances of 1.86 Å. This (4+1) coordination is one of the characteristic environments for the V^{5+} cation (Schindler et al. 2000). Potassium atoms were found to be coordinated in distinct ways in the mathesiusite structure. The K1 atom is [9]-coordinated with an average bond length ~3 Å, while the K2 atom is [12]-coordinated and the average K-O bond length is higher, ~3.2 Å (Table 6). Both potassium atoms are linked to the only symmetrically unique H_2O molecule in the structure (O3 atom, see Table 7).

Structure formula

The results of the bond-valence analysis of the mathesiusite structure (Table 7) confirmed the valence states expected for the cations based on the characteristic coordinations. The calculated bond-valence sums are in agreement with the expected values for U^{6+}, K^+, S^{6+}, and V^{5+}. The O atom that belongs to the H_2O molecule is indicated by the low sum of the bond-valence incident at the O3

Table 3. Summary of data collection conditions and refinement parameters for mathesiusite

Structural formula	$K_{4.92}(UO_2)_4(SO_4)_4(VO_5)(H_2O)_4$
Unit-cell parameters	a = 14.9704(10), c = 6.8170(5) Å
V	1527.78(18)
Z	2
Space group	$P4/n$
D_{calc} (g/cm^3)	4.023 (for the formula given above)
Temperature	300 K
Radiation (wavelength)	Mo$K\alpha$ (0.7107 Å)
Crystal dimensions	0.07 × 0.02 × 0.02 mm
Collection mode	ω scans to cover the Ewald sphere
Frame width, counting time	0.8°, 200 s
Limiting θ angles	3.00–29.30°
Limiting Miller indices	$-18 < h < 19$, $-19 < k < 20$, $-9 < l < 8$
No. of reflections	12825
No. of unique reflections	1861
No. of observed reflections (criterion)	795 [$I > 3\sigma(I)$]
μ (mm^{-1}), method	22.48, combined [multi-scan and analytical, Clark and Reid (1995)]
T_{min}/T_{max}	0.391/0.662
Coverage, R_{int}	0.9982, 0.189
F_{000}	1628
Refinement	Full matrix least-squares by Jana2006 on F^2
Parameters refined	69
R_1, wR_2 (obs)	0.0519, 0.0887
R_1, wR_2 (all)	0.1567, 0.1277
GOF (obs, all)	1.09, 1.01
Weighting scheme	$1/[\sigma^2(F) + 0.0001F^2]$
$\Delta\rho_{min}$, $\Delta\rho_{max}$ (e/Å^3)	–6.07, 7.37 (near U atom)[a]

[a] The high difference Fourier maxima probably caused by the contribution of the split domains. Introduction of the twin laws did not lead to a better fit.

Table 4. Atomic positions and displacement parameters (U_{eq}, U_{iso}, in Å^2) for the crystal structure of mathesiusite

Atom	Wyckoff site	x/a	y/b	z/c	U_{eq}/U_{iso} (Å^2)
U	8g	0.30867(5)	0.06729(5)	0.12671(11)	0.0204(2)
V	2c	0.5	0	0.3172(9)	0.0221(18)
S	8g	0.8012(3)	0.1424 (3)	0.1239(8)	0.0228(15)
K1[b]	8g	0.1192(3)	0.3016 (4)	0.3777(8)	0.048(2)
K2[b]	2a	0	0	0	0.090(8)
O1	8g	0.8073(9)	0.0449 (9)	0.157(2)	0.031(4)[a]
O2	8g	0.3386(8)	0.0413 (8)	–0.1174(19)	0.022(3)[a]
O3	8g	0.0032(13)	0.1373(14)	0.386(4)	0.085(7)[a]
O4	8g	0.2765(8)	0.0956 (8)	0.3653(19)	0.023(3)[a]
O5	8g	0.8722(10)	0.1677(10)	–0.0053(17)	0.026(4)[a]
O6	8g	0.7172(10)	0.1604(10)	0.0207(18)	0.030(4)[a]
O7	8g	0.3910(8)	–0.0478(9)	0.2390(19)	0.022(3)[a]
O8	8g	0.8036(9)	0.1903(9)	0.3066(19)	0.031(4)[a]
O9	2c	0.5	0	0.555 (4)	0.032 (7)[a]

[a] Refined isotropically.
[b] Refined occupancies are 0.994(16) and 0.94(5) for K1 and K2, respectively.

[1] Deposit item AM-14-411, CIF. Deposit items are stored on the MSA web site and available via the *American Mineralogist* Table of Contents. Find the article in the table of contents at GSW (ammin.geoscienceworld.org) or MSA (www.minsocam.org), and then click on the deposit link.

TABLE 5. Anisotropic displacement parameters (Å^2) for mathesiusite

Atom	U_{11}	U_{22}	U_{33}	U_{12}	U_{13}	U_{23}
U	0.0185(4)	0.0183(4)	0.0244(4)	−0.0004(3)	0.0002(4)	0.0000(4)
V	0.020(2)	0.020(2)	0.026(4)	0	0	0
S	0.021(3)	0.016(2)	0.031(3)	−0.0004(19)	0.000(3)	0.001(3)
K1	0.044(4)	0.067(4)	0.032(3)	−0.016(3)	−0.002(3)	0.006(3)
K2	0.063(9)	0.063(9)	0.144(19)	0	0	0

TABLE 6. Selected interatomic distances (in Å) for mathesiusite

U–O1^{i}	2.425(13)	V–O7	1.859(13)
U–O2	1.767(13)	V–O7^{i}	1.859(13)
U–O4	1.748(13)	V–O7^{iii}	1.859(13)
U–O5^{ii}	2.442(14)	V–O7^{iv}	1.859(13)
U–O6^{iii}	2.402(15)	V–O9	1.62(3)
U–O7	2.252(13)	<*V–O*>	1.81
U–O7^{iv}	2.365(13)		
<*U–O$_{Ur}$*>	1.758	S–O1	1.479(14)
<*U–O$_{eq}$*>	2.377	S–O5	1.432(14)
		S–O6	1.465(15)
		S–O8	1.439(14)
		<*S–O*>	1.45
K1–O2^{vi}	3.013(14)	K2–O1^{xi}	3.149(13)
K1–O2^{vii}	3.038(14)	K2–O1^{i}	3.149(13)
K1–O3	3.01(2)	K2–O1^{ii}	3.149(13)
K1–O4^{viii}	2.805(14)	K2–O1^{xii}	3.149(13)
K1–O6^{ii}	2.801(14)	K2–O3	3.34(2)
K1–O7^{ix}	3.124(14)	K2–O3^{xiii}	3.34(2)
K1–O8^{iii}	2.893(15)	K2–O3^{xiv}	3.34(2)
K1–O8^{x}	2.870(14)	K2–O3^{vii}	3.34(2)
K1–O9^{viii}	3.495(7)	K2–O5^{xi}	3.155(14)
<*K1–O*>	3.00	K2–O5^{i}	3.155(14)
		K2–O5^{ii}	3.155(14)
O1–O2^{i}	3.152(18)	K2–O5^{xii}	3.155(14)
O1–O3^{xv}	3.29(3)	<*K2–O*>	3.22
O1–O4^{i}	2.833(18)		
O1–O5	2.353(19)	O4–O5^{ii}	2.985(18)
O1–O5^{xvi}	2.81(2)	O4–O6^{iii}	3.118(19)
O1–O6	2.38(2)	O4–O7	2.879(18)
O1–O7^{i}	3.022(18)	O4–O7^{iv}	2.775(18)
O1–O8	2.404(19)	O4–O8^{iii}	3.178(18)
O2–O5^{ii}	2.989(18)	O4–O8^{x}	2.990(18)
O2–O6^{i}	3.270(19)	O5–O6	2.33(2)
O2–O6^{iii}	2.797(19)	O5–O6^{v}	2.90(2)
O2–O7	2.880(18)	O5–O8	2.386(18)
O2–O7^{iv}	3.133(18)	O6–O6^{v}	2.87(2)
O2–O8^{ii}	3.463(18)	O6–O7^{i}	2.771(19)
O2–O9^{xvii}	3.35(2)	O6–O8	2.382(19)
O3–O3^{xviii}	3.30(3)	O6–O8^{v}	3.176(19)
O3–O3^{ix}	3.30(3)	O7–O7^{iii}	2.518(18)
O3–O4^{ix}	3.07(3)	O7–O7^{iv}	2.518(18)
O3–O5^{xi}	3.34(3)	O7–O9	2.79(2)
O3–O8^{xi}	3.14(2)		

Note: Symmetry codes: (i) *–x*+1, *–y*, *z*; (ii) *y*, *–x*+1, *–z*; (iii) *–y*+1/2, *x*–1/2, *z*; (iv) *y*+1/2, *–x*+1/2, *z*; (v) *–x*+3/2, *–y*+1/2, *–z*; (vi) *–x*+1/2, *–y*+1/2, *–z*; (vii) *–y*, *x*, *–z*; (viii) *–x*+1/2, *–y*+1/2, *–z*+1; (ix) *–y*, *x*, *–z*+1; (x) *y*, *–x*+1, *–z*+1; (xi) *x*–1, *y*, *z*; (xii) *–y*, *x*–1, *–z*; (xiii) *–x*, *–y*, *z*; (xiv) *y*, *–x*, *–z*; (xv) *–y*+1, *x*, *–z*+1; (xvi) *–y*+1, *x*–1, *–z*; (xvii) *x*, *y*, *z*–1; (xviii) *y*, *–x*, *–z*+1.

TABLE 7. The bond-valence analysis for mathesiusite (v.u.)

	U	V	S	K1	K2	ΣBV
O1	0.47		1.48		0.06 ×4↓	2.02
O2	1.72			0.09 ×2↓		1.90
O3				0.09	0.04 ×4↓	0.14
O4	1.79			0.16		1.95
O5	0.46		1.68		0.06 ×4↓	2.20
O6	0.50		1.54	0.16		2.20
O7	0.67, 0.53	0.86 ×4		0.07		2.13
O8			1.65	0.13, 0.14		1.91
O9		1.64		0.03		1.66
ΣBV	6.14	5.08	6.35	0.96	0.67	

Notes: Values are expressed in valence units (v.u.). ΣBV = bond-valence sum. U^{6+}–O bond strengths (r_0 = 2.045, b = 0.51) from Burns et al. (1997); K^{+}–O, S^{6+}–O, V^{5+}–O bond strengths from Brown and Altermatt (1985).

site. The structure formula obtained from the refinement, including the refined occupancies of the K sites, is $K_{4.92}(UO_2)_4(SO_4)_4(VO_5)(H_2O)_4$, Z = 2 (see Discussion for comments).

Structure connectivity

The structure of mathesiusite consists of sheets that are built of $[(UO_2)_4(SO_4)_4(VO_5)]^{5-}$ clusters (designated *USV*) (Figs. 3a and 4a). These clusters arise from linkage between corner-sharing quartets of uranyl pentagonal bipyramids, which define a square-shaped void at the center. These voids are occupied by V^{5+} cations (Fig. 3a). The square defined by the four equatorial O atoms is the base of the square pyramid, with the fifth O atom pointing up or down relative to the sheets (Figs. 3a and 3b). Each pair of uranyl pentagonal bipyramids shares two vertices of SO_4 tetrahedra. Each tetrahedron shares a third vertex with another *USV* to form sheets. The fourth vertex of the tetrahedron remains free, pointing up or down (Figs. 4a and 4c). The sequence of tetrahedral units in mathesiusite is …*ududud*… (*u* = up or *d* = down). The structure possesses corrugated heteropolyhedral sheets that are stacked perpendicular to *c* (Fig. 3b). The round voids defined by four *USV* are occupied by K2 and O3 atoms. The K1 atom is localized in between the corrugated sheets (Fig. 3b). Adjacent structure sheets are linked through the K–O bonds and also by hydrogen bonds.

DISCUSSION

Several issues warrant discussion. The discrepancy between the ideal formula and the chemical composition of mathesiusite, obtained from the electron microprobe analysis and X-ray diffraction is of interest. We point out that we had considerable problems with the stoichiometry obtained from the first electron microprobe study we undertook. Even if a low-beam current and wide beam-size were used, the stoichiometry of the K content was not satisfactory due to the partial K-loss from the analyzed grains. The stoichiometry from the analyses corresponded to ~4.1–4.3 K apfu only. Therefore, we used extrapolation of the polynomial quadratic fit of the K *K*α counting statistics into the t = 0 instead of counting an integral signal (Fig. 5). Using that approach we were able to derive a more reasonable stoichiometry of the compound used in the mineral proposal and presented here. During the first 8 s of the analysis the number of K *K*α counts decreases to 80 rel%, indicating the loss of 1/5 of the K content. We conclude that the partial K-loss is connected to the K2 atom in the structure, as it is located in the channel defined by the four *USV*. The U_{eq} of K2 is quite large, suggesting atomic displacements along the channel axis. We have based our conclusion about loss of the weakly bonded K2 atom, because it sits on the 2*a* site in the structure (corresponds to 1 K apfu). The refined occupancies provided similar contents: 4.92 K apfu (X-ray), 4.87 K apfu (EPMA). However, the refined occupancies might also be affected by the poor absorption correction applied to the data.

Topology of the structure

The structure topology found in mathesiusite is unique among uranyl oxysalt minerals (Fig. 4b). However, uranyl heteropolyhedral sheets of the same topology have been found in synthetic uranyl chromates prepared by Unruh et al. (2012). The fundamental building block, the tetramer of corner sharing uranyl pentagonal bipyramids, the *USqPy* cluster (where *SqPy* = V^{5+} in

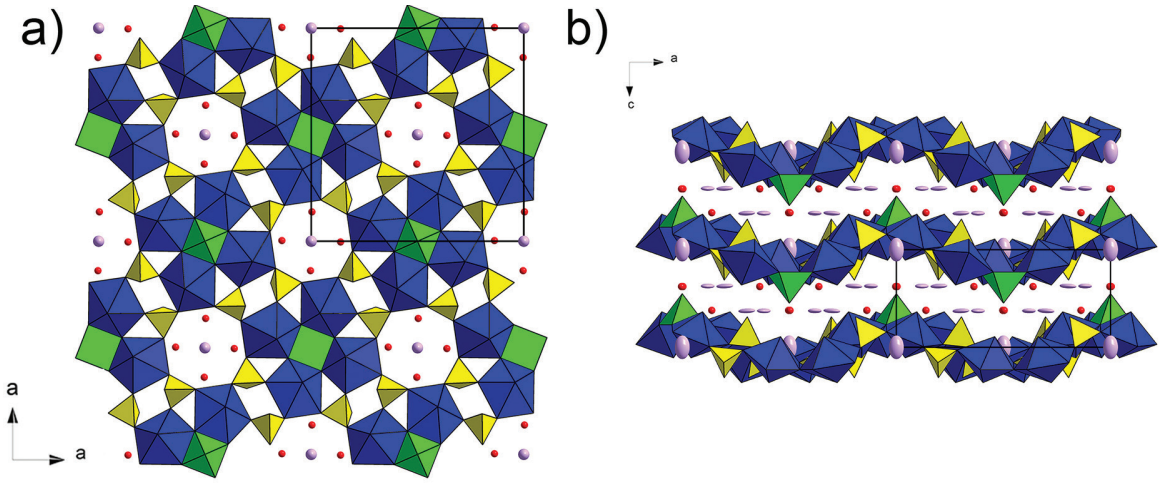

Figure 3. Crystal structure of mathesiusite. (**a**) Heteropolyhedral sheets composed of clusters of uranyl pentagonal bipyramids (blue), SO_4 groups (yellow), and VO_5 pyramids (green) viewed along [001]. The K2 atom located in the channels (pink) together with O3 (H_2O) atom (red). (**b**) The corrugated sheets of in the structure with K^+ cations and H_2O (red) in the interlayer. Viewing direction along [010].

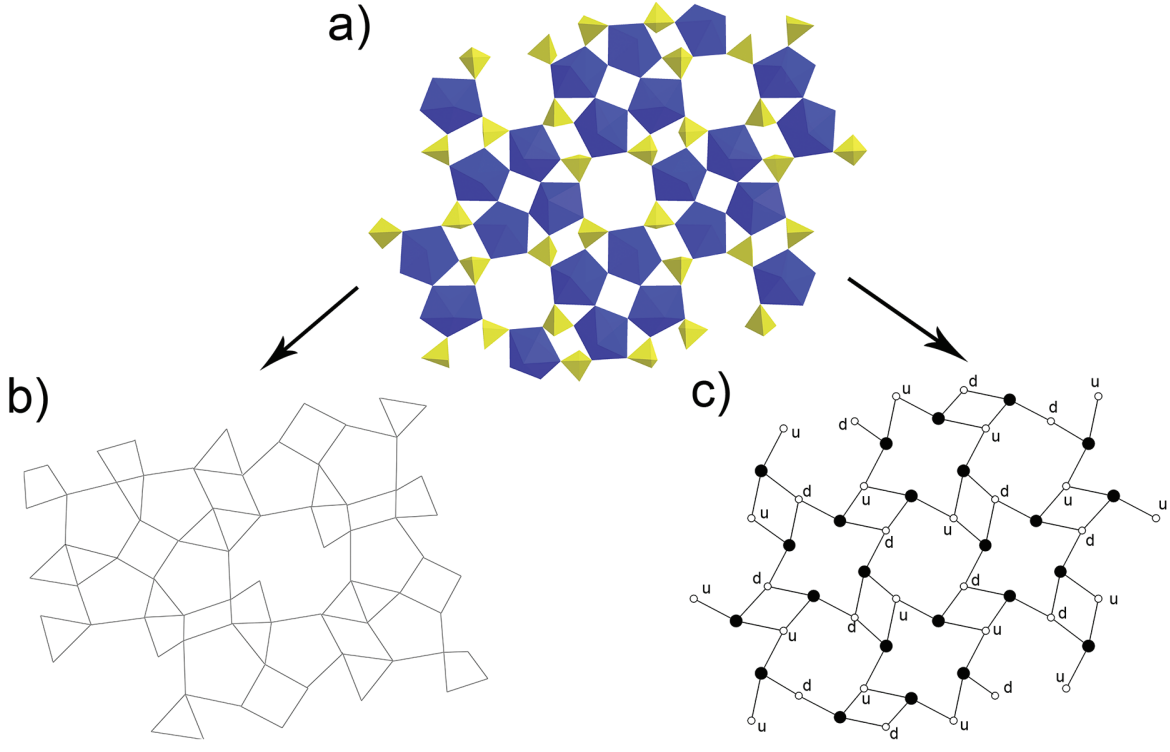

Figure 4. The topology of the structural sheet of polyhedra in mathesiusite. (**a**) Polyhedral representation of uranyl sulfate sheet. (**b**) Its topology represented by graph, based upon pentagons, squares, and triangles. (**c**) The graph of mathesiusite topology with respective orientation (*u* = up or *d* = down) of the tetrahedral anions.

case of mathesiusite) was found also in other inorganic uranyl compound, such as synthetic $Cs_6[(UO_2)_4(W_5O_{21})(OH)_2(H_2O)_2]$ (Sykora et al. 2004), which anyway is the topological isomer. Unruh et al. (2012) provided the complex crystallographic study of the three novel uranyl chromates, $Li_5[(UO_2)_4(Cr^{5+}O_5)(Cr^{6+}O_4)_4](H_2O)_{17}$, $[Mg(H_2O)_6]_5[(UO_2)_8(Cr^{5+}O_5)_2(Cr^{6+}O_4)_8]$, and $(NH_4)_5[(UO_2)_4(Cr^{5+}O_5)(Cr^{6+}O_4)_2]H_2O_{11}$. All three phases are triclinic ($P\bar{1}$) and have similar unit-cell volumes. All three phases have sheets of polymerized polyhedra based upon the same topology. However, these sheets differ in the orientation of the tetrahedral elements, a phenomenon that is called graphical isomerism (Krivovichev 2010). The following two graphical isomers were resolved between the above mentioned compounds: …*ududud*… (Li- and NH_4-containing compound of Unruh et al. 2012), and …*uudduu*… (Mg-containing

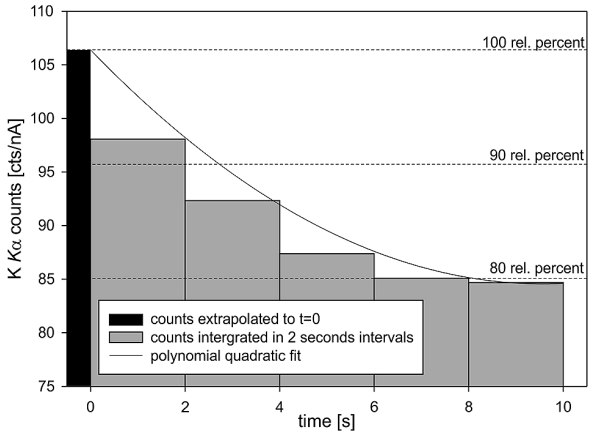

FIGURE 5. Plot shows the loss of potassium during the electron microprobe analysis. The K *K*a peak counting time (10 s) was divided into five 2 s intervals. The number of counts from each interval is plotted (an average of 5 analyses). The theoretical potassium content before beginning of the analysis was calculated by extrapolation of quadratic polynomial fit to the time $t = 0$ s. Note the content of K decreases to 80 rel% after 8 s.

compound of Unruh et al. 2012; Figs. 6a and 6b). Mathesiusite belongs to the first group where *T* elements alternate regularly up and down.

The bond-valence approach to the structure of mathesiusite

The bond-valence approach is a simple framework for considering crystal-chemical relations of solids by means of the bond-valence method developed by Brown (1981, 2002, 2009). The so-called bond-valence approach was introduced and developed by Hawthorne and Schindler to assess, explain, and estimate some of the stereochemical behavior of the namely hydrous oxysalt minerals (Hawthorne 1992, 2012; Hawthorne and Schindler 2008; Schindler and Hawthorne 2008; Hawthorne and Sokolova 2012). Here we consider the hydrated uranyl oxysalt mineral mathesiusite as a binary structure, consisting of a strongly bonded structural unit (s.u.), $[(UO_2)_4(SO_4)_4(VO_5)]^{5-}$, apparently having anionic character (Lewis base), and a weakly bonded complex occupying the interlayer space, $[^{[12]}K^{[9]}K_4(H_2O)_4]^{5+}$, having cationic character (Lewis acid). According to the principle of correspondence (Schindler and Hawthorne 2008), which is the mean-field equivalent of the valence-matching principle (Brown 1981, 2002), stable structures will form when the value of Lewis basicity closely matches the value of Lewis acidity, meaning that the interlayer complex is "compatible" with the structural unit in terms of the type of cation, number of bonds to the structure unit, number of H-bond acceptors within the structure unit, number of H_2O in the interlayer and the type according to their role in the bond-valence transfer. We will not recall all the details and terminology, as they can be found in the above mentioned papers.

The structural unit of mathesiusite can be written in the reduced form as $[(UO_2)(SO_4)(VO_5)_{0.25}]^{1.25-}$, which contains 7.25 anions. This unit is characterized by the charge deficiency per anion, *CDA*, of (1.25/7.25) = 0.17 v.u. As was demonstrated elsewhere (Hawthorne and Schindler 2008; Schindler and Hawthorne 2008) the *CDA* closely correlates with the mean coordination number of the O atoms within the structural units, respectively with the number of bonds per anion received from the interstitial complex and adjacent structural unit, and can thus can be used to predict the minimum and maximum number of bonds, which can be accepted by the structural unit. This range of bonds defines the range in Lewis basicity of the structural as it is defined as the charge of the structural unit divided by the number of accepted bonds (Brown 2002). Using the correlation between the *CDA* and the coordination number for O, the calculated range (min–max) in number of bonds required by the structural unit is 5 and 9. The corresponding range of Lewis basicity is 0.15–0.26 v.u. Let us consider next the interstitial complex, $\{^{[12]}K_{0.25}{}^{[9]}K(H_2O)\}^{1.25+}$. We need to inspect the coordination environment around K atoms carefully in order determine its Lewis acidity, which is defined as the charge of the complex divided by the number of emanated bonds toward the structural unit. The K1 site is [8]-coordinated, however, only 7 bonds link K1 atoms to the structural unit directly (at the distance of 3.25 Å). The eighth ligand is the H_2O site (O3 atom), which will be discussed later. The K2 atom is [8]-coordinated at the distance of 3.25 Å and all these bonds link the K2 atom to the shared O atoms between uranyl pentagonal bipyramids and SO_4 groups (O1 and O5, see Table 6). However, K2 is linked by weak bonds to O3 (H_2O) at a distance of ~3.3 Å. The O3 atom, which belongs, according to the bond-valence analysis (0.14 v.u.), to

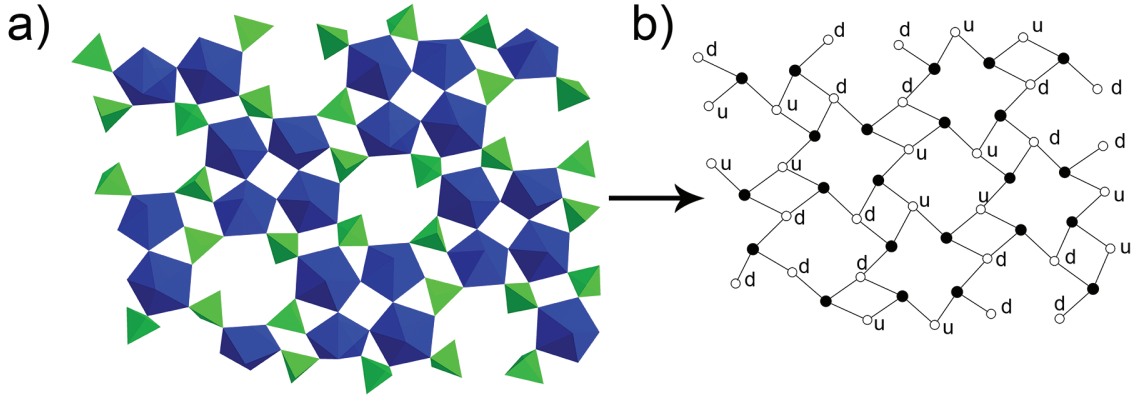

FIGURE 6. The topology of the structural sheet of polyhedra in synthetic Mg-dominant uranyl chromate (Unruh et al. 2012). (**a**) Polyhedral representation of uranyl chromate sheet ($Cr^{5+}O_5$ groups omitted). (**b**) The graph representation with respective orientation (*u* = up or *d* = down) of the tetrahedral anions.

a H_2O group, is [5]-coordinated, receiving one bond from each of the K1 and K2 atoms, donating 2 bonds to corresponding H atoms and receiving bonds from K1, K2, and two hydrogen atoms as well as a hydrogen bond from its corresponding symmetrical equivalent [theoretical BV sums for O3 with calculated contributions from H-bonds: 0.09 (K1) + 0.04 (K2) + 2×0.80 as H-donor + 0.20 as H-acceptor = 1.93 v.u.]. Hence, the O3 atom belongs to an inverse-transformer (H_2O) group, which rarely occurs in the structure of minerals (Hawthorne 1992; Schindler and Hawthorne 2008), and is usually bonded to monovalent cations occurring in coordination numbers higher than [7] (Schindler and Hawthorne 2008). Theoretically, by the action of one inverse-transformer (H_2O) group one bond is removed from the bonding scheme between the interstitial complex and structural unit (Schindler and Hawthorne 2008). Hence, the total number of emanated by the interstitial complex is 40, the corresponding Lewis acidity can be calculated as 0.17 v.u., which matches the range in Lewis basicity of the structural unit. Schindler and Hawthorne (2008) presented an empirical relation between the number of anions in structural units of uranyl-sheet minerals and the number of bonds emanating from the interstitial complex, the number of OH groups emanated from the structural unit and the number and the type of interstitial (H_2O) groups. Based on these empirical relations, using a so called bond-valence distribution factor (D), one can calculate the total number of (H_2O) groups per cation and the number of interstitial transformer (H_2O) groups. We derived a D factor for mathesiusite, which is equal to ~0.66. Using Equation 7 of Schindler and Hawthorne (2008), the number of transformer (H_2O) groups in the interstitial complex should be –1. It means that there should be more non-transformer or inverse-transformer (H_2O) groups in mathesiusite than transformer (H_2O) groups. This is in accordance with the observed structure.

Acknowledgments

The authors are grateful to Ladislav Lapčák (Institute of Chemical Technology, Prague) for help with Raman spectroscopic analysis. We thank Peter Burns for drawing our attention to the structures of synthetic uranyl chromates. The manuscript benefited from the comprehensive thorough reviews of the three anonymous referees and from the careful editorial handling of Fernando Colombo. This research was financially supported by the Premium Academie Grant of the ASCR, v.v.i., by the post-doctoral Grant of the GACR no. 13-31276P to J.P., and by the project DKRVO 2013/02 and 2014/02 (National Museum, 00023272) of the Ministry of Culture of the Czech Republic for J.S. and J.Č.

References cited

Agilent Technologies (2012) CrysAlis CCD and CrysAlis RED. Oxford Diffraction, Yarnton, Oxfordshire, U.K.

Bartlett, J.R., and Cooney, R.P. (1989) On the determination of uranium-oxygen bond lengths in dioxouranium(VI) compounds by Raman spectroscopy. Journal of Molecular Structure, 193, 295–300.

Brown, I.D. (1981) The bond-valence method: An empirical approach to chemical structure and bonding. In M. O'Keeffe and A. Navrotsky, Eds., Structure and Bonding in Crystals II, p. 1–30. Academic Press, New York.

——— (2002) The Chemical Bond in Inorganic Chemistry: The bond valence model. Oxford University Press, U.K.

——— (2009) Recent developments in the methods and applications of the bond valence model. Physical Review, 109, 6858–6919.

Brown, I.D., and Altermatt, D. (1985) Bond-valence parameters obtained from a systematic analysis of the inorganic crystal structure database. Acta Crystallographica, B41, 244–247. URL: http://www.iucr.org/resources/data/data-sets/bond-valence-parameters (Accessed: 2014-01-16; archived by WebCite at http://www.webcitation.org/6MfL4QtPE).

Burns, P.C. (2005) U^{6+} minerals and inorganic compounds: Insights into an expanded structural hierarchy of crystal structures. Canadian Mineralogist, 43, 1839–1894.

Burns, P.C., Ewing, R.C., and Hawthorne, F.C. (1997) The crystal chemistry of hexavalent uranium: Polyhedron geometries, bond-valence parameters, and polymerization of polyhedra. Canadian Mineralogist, 35, 1551–1570.

Chernorukov, N.G., Suleymanov, E.V., Knyazev, A.V., Vyshinski, N.N., and Klimov, E.Y. (2000) Vibrational spectra of uranyl vanadates of mono- and divalent metals. Zhurnal Obshchey Khimii, 70, 1418–1424.

Clark, R.C., and Reid, J.S. (1995) The analytical calculation of absorption in multifaceted crystals. Acta Crystallographica, A51, 887–897.

Hawthorne, F.C. (1992) The role of OH and H_2O in oxide and oxysalt minerals. Zeitschrift für Kristallographie, 201, 183–206.

——— (2012) A bond-topological approach to theoretical mineralogy: Crystal structure, chemical composition and chemical reactions. Physics and Chemistry of Minerals, 39, 841–874.

Hawthorne, F.C., and Schindler, M. (2008) Understanding the weakly bonded constituents in oxysalt minerals. Zeitschrift für Kristallographie, 223, 41–68.

Hawthorne, F.C., and Sokolova, E. (2012) The role of H_2O in controlling bond topology: I. The $^{[6]}Mg(SO_4)(H_2O)_n$ (n = 0–11) structures. Zeitschrift für Kristallographie, 227, 594–603.

Knyazev, A.V. (2000) Synthesis, structure and properties of uranyl vanadates of mono-, di- and trivalent metals. Ph.D. thesis, N.I. Lobachevsky State University of Nizhny Novgorod, Russia.

Kraus, W., and Nolze, G. (1996) POWDER CELL—A program for the representation and manipulation of crystal structures and calculation of the resulting X-ray powder patterns. Journal of Applied Crystallography, 29, 301–303.

Krivovichev, S.V. (2010) Actinyl compounds with hexavalent elements (S, Cr, Se, Mo)—structural diversity, nanoscale chemistry, and cellular automata modelling. European Journal of Inorganic Chemistry, 2010, 2594–2603.

Laugier, J., and Bochu, B. (2004) LMPG Suite of Programs for the interpretation of X-ray Experiments. ENSP/Laboratoire des Matériaux et du Génie Physique, BP 46. 38042 Saint Martin d'Hères, France. URL: http://www.ccp14.ac.uk/tutorial/lmgp/ (Accessed: 2014-01-16).

Ondruš, P., Veselovský, F., Skála, R., Císařová, I., Hloušek, J., Frýda, J., Vavřín, I., Čejka, J., and Gabašová, A. (1997) New naturally occurring phases of secondary origin from Jáchymov (Joachimsthal). Journal of the Czech Geological Society, 42, 77–108.

Ondruš, P., Veselovský, F., Gabašová, A., Hloušek, J., Šrein, V., Vavřín, I., Skála, R., Sejkora, J., and Drábek, M. (2003) Primary minerals of the Jáchymov ore district. Journal of the Czech Geological Society, 48, 3-4, 19–147.

Oszlányi, G., and Süto, A. (2004) Ab-initio structure solution by charge flipping. Acta Crystallographica, A, 60, 134–141.

——— (2008) The charge flipping algorithm. Acta Crystallographica, A, 64, 123–134.

Palatinus, L. (2013) The charge-flipping algorithm in crystallography. Acta Crystallographica, B, 69, 1–16.

Palatinus, L., and Chapuis, G. (2007) Superflip – A computer program for the solution of crystal structures by charge flipping in arbitrary dimensions. Journal of Applied Crystallography, 40, 451–456.

Petříček, V., Dušek, M., and Palatinus, L. (2006) Jana2006. The crystallographic computing system. Institute of Physics, Praha, Czech Republic.

Plášil, J., Hloušek, J., Veselovský, F., Fejfarová, K., Dušek, M., Škoda, R., Novák, M., Čejka, J., Sejkora, J., and Ondruš, P. (2012) Adolfpateraite $K(UO_2)(SO_4)(OH)(H_2O)$, a new uranyl sulphate mineral from Jáchymov, Czech Republic. American Mineralogist, 97, 447–454.

Pouchou, J.L., and Pichoir, F. (1985) "PAP" (φρZ) procedure for improved quantitative microanalysis. In J.T. Armstrong, Ed., Microbeam Analysis, 104–106. San Francisco Press, California.

Schindler, M., and Hawthorne, F.C. (2008) The stereochemistry and chemical composition of interstitial complexes in uranyl-oxysalt minerals. The Canadian Mineralogist, 46, 467–501.

Schindler, M., Hawthorne, F.C., and Baur, W.H. (2000) Crystal chemical aspects of vanadium: polyhedral geometries, characteristic bond valences, and polymerization of (VO_n) polyhedra. Chemistry of Materials, 12, 1248–1259.

Sykora, R.E., McDaniel, S.M., and Albrecht-Schmitt, T.E. (2004) Hydrothermal synthesis and structure of $K_6[(UO_2)_4(CrO_4)_7]\,6H_2O$: A layered uranyl chromate with a new uranyl sheet topology. Journal of Solid State Chemistry, 177, 1431–1436.

Unruh, D.K., Quicksall, A., Pressprich, L., Stoffer, M., Qiu, J., Nuzhdin, K., Wub, W., Vyushkova, M., and Burns, P.C. (2012) Synthesis, characterization, and crystal structures of uranyl compounds containing mixed chromium oxidation states. Journal of the Solid State Chemistry, 191, 162–166.

Manuscript received July 23, 2013
Manuscript accepted November 27, 2013
Manuscript handled by Fernando Colombo